PERGAMON

Electrochimica Acta 45 (2000) 3213–3223

ELECTROCHIMICA Acta

www.elsevier.nl/locate/electacta

STM measurement of current–potential curves at a semiconductor surface

R. Hiesgen [a,*], M. Krause [b], D. Meissner [c]

[a] *Physikdepartment E19, Technische Universität München, James-Franck-Strasse 1, D-85748 Garching, Germany*
[b] *Forschungszentrum Jülich, ISI, D-52425 Jülich, Germany*
[c] *Physikalische Chemie, Technische Universität Linz, Altenberger Strasse 69, A-4040 Linz, Austria*

Received 14 November 1999; received in revised form 14 January 2000

Abstract

A new experimental method for the analysis of current–potential curves determined with a scanning tunneling microscope in an electrochemical cell is described. Spectroscopic measurements have been performed in sulfuric acid at a tungsten diselenide semiconductor sample. Measurements of current–voltage curves obtained with the STM for different tunneling gaps and for different potentials of the tip and the semiconductor are recorded, and results are shown. Current–distance curves obtained from these measurements allow the separation of the influence of the tunneling barrier from that of the Schottky barrier at the semiconductor/electrolyte interface. Changes in the barrier heights are due to an electronic influence from the tip potential on the semiconductor surface potential when the tip enters the electrochemical double layer.

Keywords: STM; Photoelectrochemistry; WSe_2; Spectroscopy; Barrier

1. Introduction

With the invention of the scanning tunneling microscope (STM) [1], it has become possible to investigate, not only the structural properties of surfaces down to atomic scale, but also a variety of physical (e.g. electronic) properties. Using semiconductor samples, ones approach is to investigate the local electronic properties by measuring the magnitude of the photocurrent at a semiconductor surface. Here, a resolution of 1 nm in the photocurrent image can be achieved [2]. The photocurrent is generated at the semiconductor surface where a large band bending is caused by the water layer present at the semiconductor surface in ambient air. The photogenerated charge carriers can be measured as a tunneling current through the STM tip. The local magnitude of the photocurrent is controlled by the position of the band edges (flatband potential) at the surface. Thereby, e.g. local space charge regions connected with surface structures like steps can be detected [3]. With this method it has also been possible to directly image the particle size dependent width of the space charge regions connected to nanosized metal contacts on a semiconductor surface [4]. This is of interest, e.g. for the catalytic influence of nanosized metal particles (multiple nano contacts: MNP) on the electron transfer in electrochemistry or photoelectrochemistry [5–7]. In ambient air the contact formed by the STM tip, the tunneling gap and the semiconductor surface behaves like a MIS (metal–insulator–semiconductor) contact [8,9]. The most important property of this contact is that the short circuit photocurrent is in a certain range independent of the distance between the tunneling tip and the semiconductor surface, which

* Corresponding author. Tel.: +49-89-28912; fax: +49-89-28912.
E-mail address: rhiesgen@ph.tum.de (R. Hiesgen)

0013-4686/00/$ - see front matter
PII: S0013-4686(00)00425-4

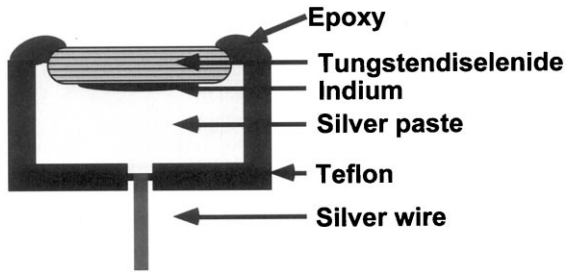

Fig. 1. Scheme of the sample holder with the semiconductor sample.

means that it is not determined by tunneling but by the transport of the charge carriers in the semiconductor.

Although measurements in ambient atmosphere have been proven to be useful for studying the electronic properties of semiconductor surfaces, more insight is expected from in-situ measurements in an electrochemical cell. Here, the potential of the semiconductor and the tunneling tip can be controlled independently. The potential of the semiconductor, with respect to a reference potential in the solution, determines the barrier at the semiconductor surface and as a result, the current over this barrier. Thereby two barriers determine the tunneling current: the tunneling barrier and the barrier at the semiconductor surface. The properties of the contact between the tip and the semiconductor formed

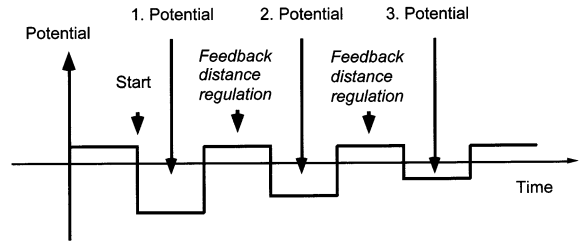

Fig. 3. Scheme of the measuring procedure for recording the current–potential curves.

under these controlled conditions are studied by measuring the tunneling current for different potentials of the tip and the semiconductor. The experimental setup for those measurements and current–potential curves obtained are discussed here. It will be shown for the first time that when the tip is inside the electrochemical double layer, the potential of the tip has a significant influence on the surface potential of the semiconductor, and therefore changes the barrier height for the tunneling current.

2. Experimental

The setup is based on a commercial STM (Nanoscope III, Digital Instruments, Santa Barbara,

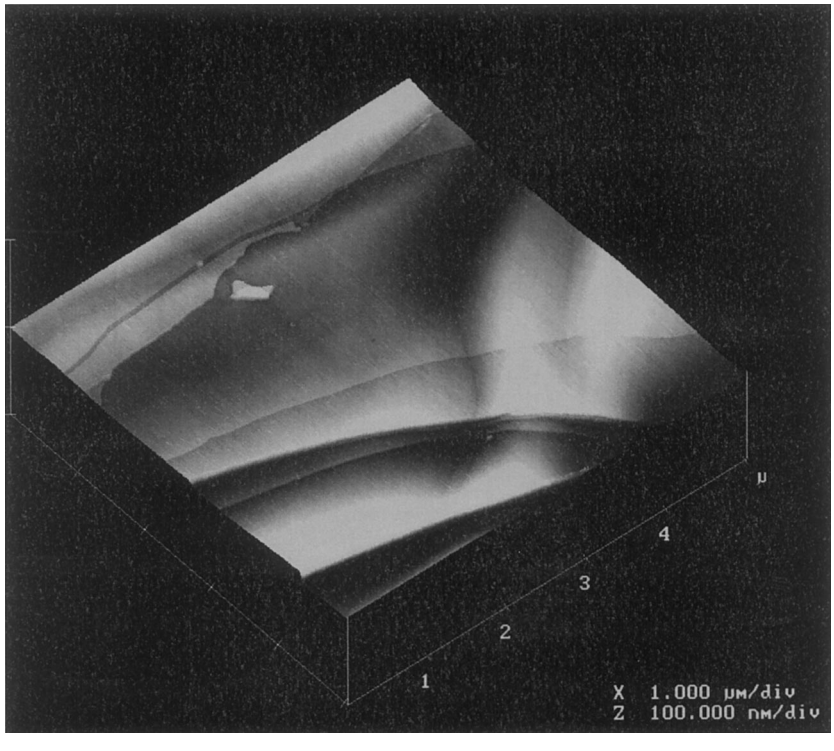

Fig. 2. STM image of an area of 5×5 μm^2 of WSe_2 recorded in air.

CA) which is equipped with a bipotentiostat. The electrochemical cell is made from Teflon. A platinum wire is used as a counter electrode and as a reference electrode, an AgCl covered silver wire is used which is frequently controlled against a standard calomel electrode. All potentials are given against this reference potential (223 mV NHE) if not mentioned otherwise. The potential of the tip and the semiconductor sample are controlled by the bipotentiostat with respect to the reference electrode. The bias voltage between sample and tip that determines the tunneling processes is defined by the difference of the two electrode potentials. All measurements reported here were performed in 0.01 M H_2SO_4. The STM is working in a closed chamber where a controlled oxygen free gas atmosphere can be maintained. As tunneling tips, electrochemically etched Pt:Ir (90:10) wires have been used after insulation with an electrophoretically applied lac-

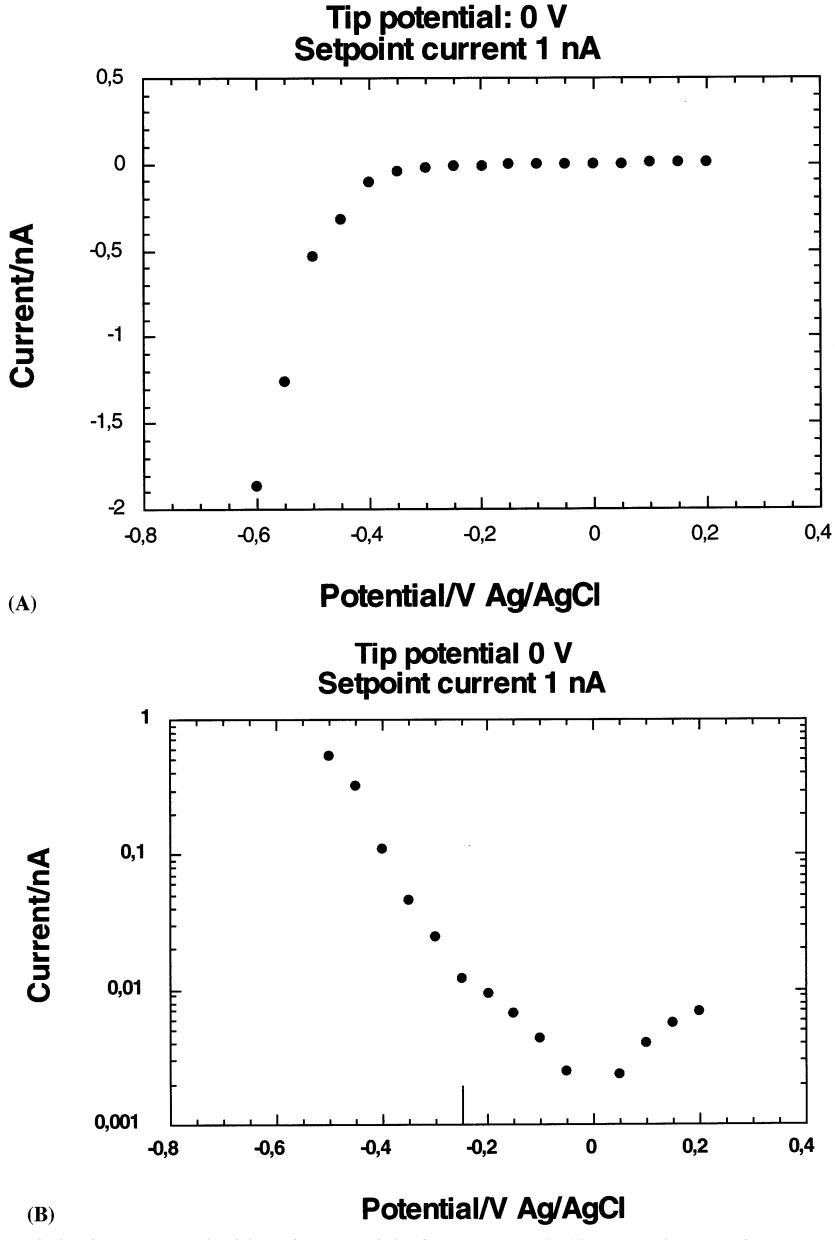

Fig. 4. Current–voltage behavior measured with a tip potential of 0 V versus Ag/AgC1 and a setpoint current of 1 nA in 0.01 m H_2SO_4: (a) linear plot of the current between the tunneling tip and the sample; (b) semilogarithmic plot of the current through the tunneling tip.

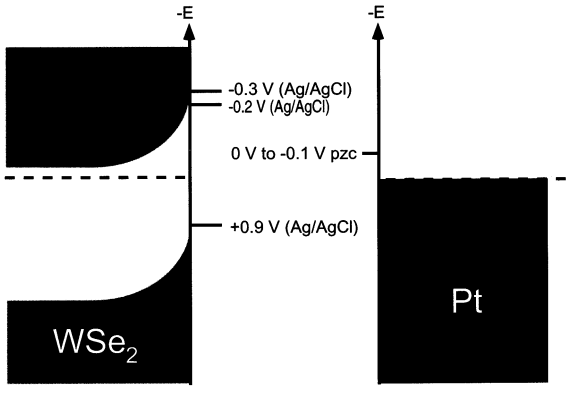

Fig. 5. Energy levels of the band edges of n-WSe_2 (left side) and the Fermi level as well as the pzc of the platinum tip (right side) in solution.

quer for minimizing the faradaic currents [10]. For polycrystalline platinum the potential of zero charge (pzc) taken from the literature is expected between $+0.11$ and $+0.27$ V NHE [11].

As a model semiconductor monocrystalline n-WSe_2 samples with doping levels of 4×10^{16} cm^{-3} have been used. This layered semiconductor can be cleaved with adhesive tape exposing large terraces of non-reactive van-der-Waals surfaces separated by only few monolayer high steps. The ohmic back contact was prepared by soldering indium to the back of the crystal and has in all cases been confirmed to be ohmic by current–voltage-measurements. The semiconductor samples were fixed to the sample holder with silver paste and the surface and the edges of the sample were covered by epoxy glue. A scheme of this arrangement is shown in Fig. 1.

WSe_2 has a bandgap of 1.2 eV. In the dark, the flatband potential has a value of -0.2 V $\pm$ 50 mV Ag/AgCl and is independent of the pH [12]. A STM image of the WSe_2 surface of an area of 5×5 μm^2 performed in air is shown in Fig. 2.

3. Current–potential curves

Current–potential curves are typically measured with an interrupted feedback method. A certain setpoint current and a bias voltage define the distance between the tunneling tip and the semiconductor and the feedback is then switched off for a short period of time. During this period the voltage is changed to the desired values and the subsequent tunneling current can be measured. After this measuring period the feedback is switched on again to establish the distance control. For the measurement of current–potential curves in our experiment the STM operation had to be controlled by an external program. This has become necessary because the built-in current–voltage procedure did not allow the use of appropriate time constants for in-situ measurements. With the external program, the setpoint tunneling current, the potentials of the tip and the semiconductor, the measuring periods and the control of the feedback regulation can be chosen freely. The current–potential curves are measured point by point in an interrupted feedback method using a separate measuring cycle for every potential. A scheme of the measuring procedure is given in Fig. 3. Between every two measured potential values, the distance between tip and semiconductor is reestablished by running the STM in feed back mode at pre defined values for current and potentials. The pre defined semiconductor potential for establishing the distance control has, in all cases, been chosen more negative than the flatband potential to assure that the forward current through the semiconductor is large enough to establish a stable tunneling. In this case, the current is controlled by the tunneling barrier and is not limited by the barrier height at the semiconductor surface.

The measurements have been performed with different tip and semiconductor potentials. The distance between tip and semiconductor has been varied by changing the setpoint current during feedback operation. The measuring time per point and the time for the feedback operation are both set to 0.3 s to establish a stationary tunneling current after the potential switch as controlled experimentally. The distance change due to thermal drift during this period has been checked separately and is negligibly small. The current through the STM tip during the measuring time and the potential for every set of parameters are then measured by two external voltmeters (Keithley 404) and stored in a separate computer.

4. Results and discussion

In Fig. 4a, a typical current–potential curve of the semiconductor is shown. Here the tip potential is held fixed at a value of 0 V vs. Ag/AgCl and the potential of the semiconductor has been varied between -0.6 and $+0.2$ V. Its diode behavior reflects the change of the barrier at the semiconductor surface with semiconductor potential. In this case, the semiconductor barrier height determines the magnitude of the electron current flowing from the semiconductor to the tip. This behavior is expected for semiconductor potentials more positive than the flatband potential (as independently determined to be at -0.2 ± 0.05 V vs. Ag/AgCl [12]).

For potentials negative of the flatband potential, a different behavior is expected. In the semilogarithmic plot in Fig. 4b, a change in the slope of the curve is visible at a potential of −0.25 V and is attributed to the expected change of behavior close to the flatband potential when the thermionic currents become very large and the current starts to be controlled by the tunneling process. A scheme of the energy levels in the electrolyte is given in Fig. 5. At more negative potentials there is no longer a barrier at the semiconductor surface and the tunneling barrier between n-WSe_2 and platinum now determines the current.

5. Electron current

In Fig. 6 current–potential curves are shown in which the semiconductor potential is varied between −0.6 V versus Ag/AgCl and +0.2 V versus Ag/AgCl with a fixed tip potential for each curve held at 0 V in Fig. 6a, +0.2 V in Fig. 6b, +0.4 V in Fig. 6c, and −0.2 V in Fig. 6d. From the plotted current values, the small faradaic current measured at zero bias voltage has been subtracted. The different curves in each figure are measured at different distances between tip and semiconductor surface realized through a different setpoint current during the feedback operation.

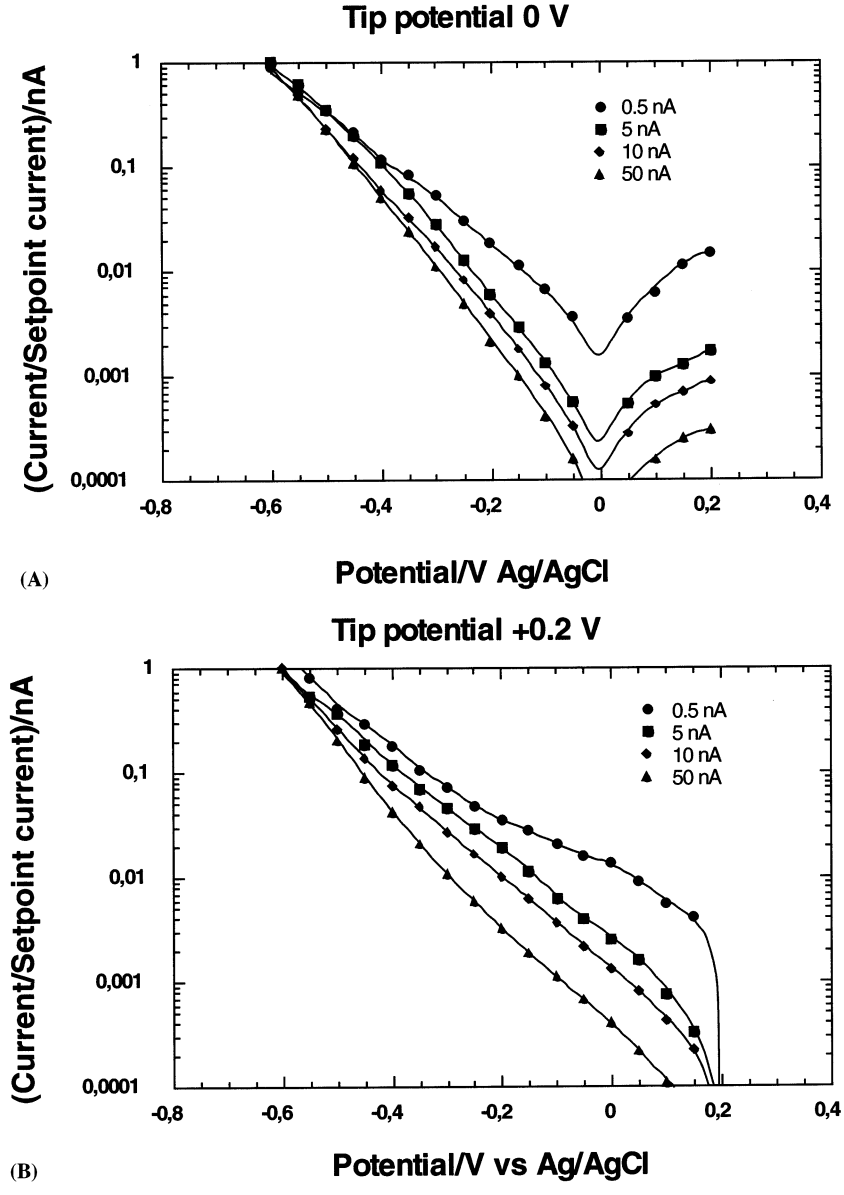

Fig. 6. Semilogarithmic plot of the normalized current through the tunneling tip versus the semiconductor potential, measured in 0.01 m H_2SO_4 recorded for different setpoint currents with a tip potential of (a) 0 V; (b) +0.2 V; (c) +0.4 V; and (d) −0.2 V.

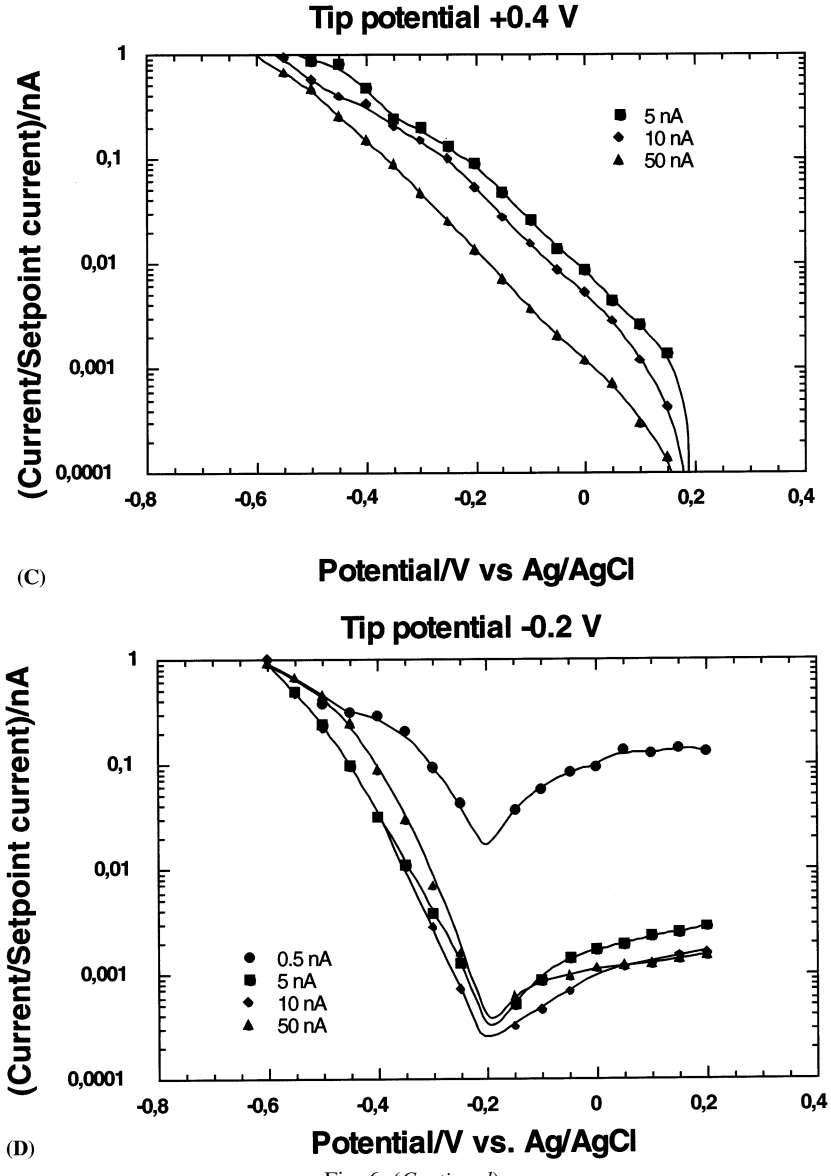

Fig. 6. (*Continued*)

For a better comparison of the curves at different distances, all current values have been divided by the magnitude of the setpoint currents (given in the figures) in order to normalize to a setpoint current of 1 nA. Assuming that only the tunneling process would determine the current, the current–potential curves for different setpoint currents should be identical after this normalization. However, as can be seen in Fig. 6, pronounced differences between the normalized current values obtained for different tip distances can be found for all tip potentials. The currents for smaller distances are typically smaller than expected for a pure tunneling determined process. In addition, the current–potential curves for the smaller setpoint currents and therefore the larger distances differ in their voltage dependence significantly from those obtained at smaller distances between tip and semiconductor (larger setpoint currents). For all tip potentials, the current–potential curves differ significantly with the setpoint current and therefore with the distance between semiconductor surface and platinum tip.

In Fig. 7 the normalized current–potential curves for the smallest distance recorded at a setpoint current of 50 nA are plotted together in one semilogarithmic plot. The slope for the curves recorded with a more negative tip potential is steeper than those recorded with more positive potentials.

The current flowing from the semiconductor to the tunneling tip has to pass two barriers: at the semiconductor surface there is an energy barrier for electrons caused by the contact with the electrolyte, and between the semiconductor surface and the tip there is a tunneling barrier which is filled with electrolyte (compare Fig. 5). For small distances one would expect that mainly the barrier in the semiconductor determines the current. At large distances between tip and semiconductor the current is mainly determined by the tunneling barrier in the gap. The height of this barrier calculated from the work functions of n-WSe_2 with about $\phi = 4.5$ eV [13] and platinum with $\phi = 5.6$ eV should be about 5 eV, neglecting the influence of the electrolyte. Due to the interaction with the solvent in the electrolyte, typically barrier heights of around 1 eV are measured [14]. The small barrier heights measured in the electrolyte are not fully understood but there are models that explain this phenomenon in principle [15]. A value of about 1 eV is also expected for a Schottky barrier formed by a solid state device of these two materials [16]. Taking this value as the tunneling barrier, the current should increase by a factor of ten for every decrease of the tunneling gap by 2.3 Å. In the limit of very small distances almost no electrolyte is expected to be inside the tunneling gap and one would expect to form a Schottky-contact between semiconductor and tip.

Changing the distance between the tip and the sample, one therefore expects to find a change in the current–potential curves which is caused by the transition between a limitation by the tunneling over the barrier in the electrolyte and a current limited by the barrier in the semiconductor. Therefore, we attribute the change in the current–potential curves with the distance to this transition.

6. Tunneling barrier

Tunneling barriers can be derived from the change in the tunneling current with distance [17]. Accordingly, if one assumes tunneling of the charge carriers over the barrier ϕ, its height can be calculated from Eq. (1):

$$\phi = 0.952(\mathrm{d}(\ln I)/\mathrm{d}s)^2 \quad (1)$$

In order to separate the influence of the two barriers involved, we study the distance behavior of the tunneling current. The measured current values have been recorded and plotted as a function of the setpoint current. The results are given in Fig. 8.

For adjusting the distance between the tip and the semiconductor, a semiconductor potential of -0.6 V vs. Ag/AgCl was chosen. At this potential the bands are already bent downwards and the electrons in the conduction band of the n-doped WSe_2 do not have to cross a barrier in the semiconductor. Therefore the only barrier in this case is the tunneling barrier. In Fig. 8, the upper curve for the semiconductor potential of -0.6 V represents the values for the setpoint current leading to a straight line. Because the distance variation has not been calibrated on an absolute scale, it is not possible to calculate the exact value of the barrier height from these measurements. However, as a measure of the distance, also the setpoint current can be taken directly. This value has been plotted on a logarithmic scale as the x-axis. Assuming a barrier in the

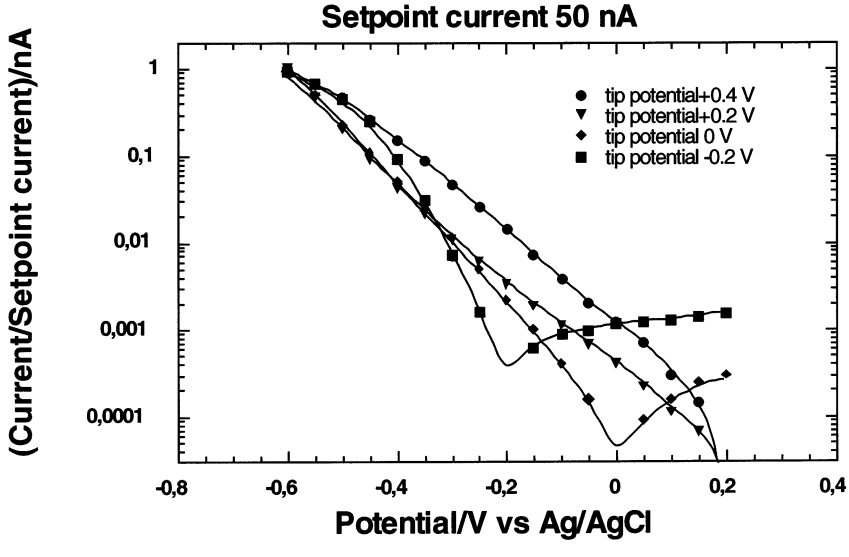

Fig. 7. Semilogarithmic: plot of the normalized current through the tunneling tip measured in 0.01 m H_2S0_4 for a setpoint current of 50 nA and different tip potentials.

electrolyte of about 1 eV [14], the distance is changing by 0.23 nm with one order of magnitude change of the setpoint current. For a constant barrier height, one expects an exponential rise of the tunneling current with smaller distance and thus a straight line in the semilogarithmic plot of the current versus distance. Currents below a value of 0.01 nA (marked by a line in the plots) are in the range of the faradaic current. Since this value was determined independently and was then subtracted from the measured values, the given data may scatter a lot and are therefore treated as a residual background.

In Fig. 8a, the current–distance curves recorded with a tip potential of 0 V are plotted for different semiconductor potentials from −0.6 to −0.20 V. All the curves have the same slope, as the upper curve indicates no change of the barrier with distance and no change of the barrier with changing the semiconductor potential. The lines drawn in Fig. 8 are given as parallel guides for the eyes and do not represent fits to the current values. In Fig. 8b the current–distance curves for different semiconductor potentials and a tip potential of +0.2 V Ag/AgCl are given. The upper curve represents the current values for the setpoint currents giving as a straight line with a slope of 1. This slope is representing the barrier attributed to the tunneling barrier in the

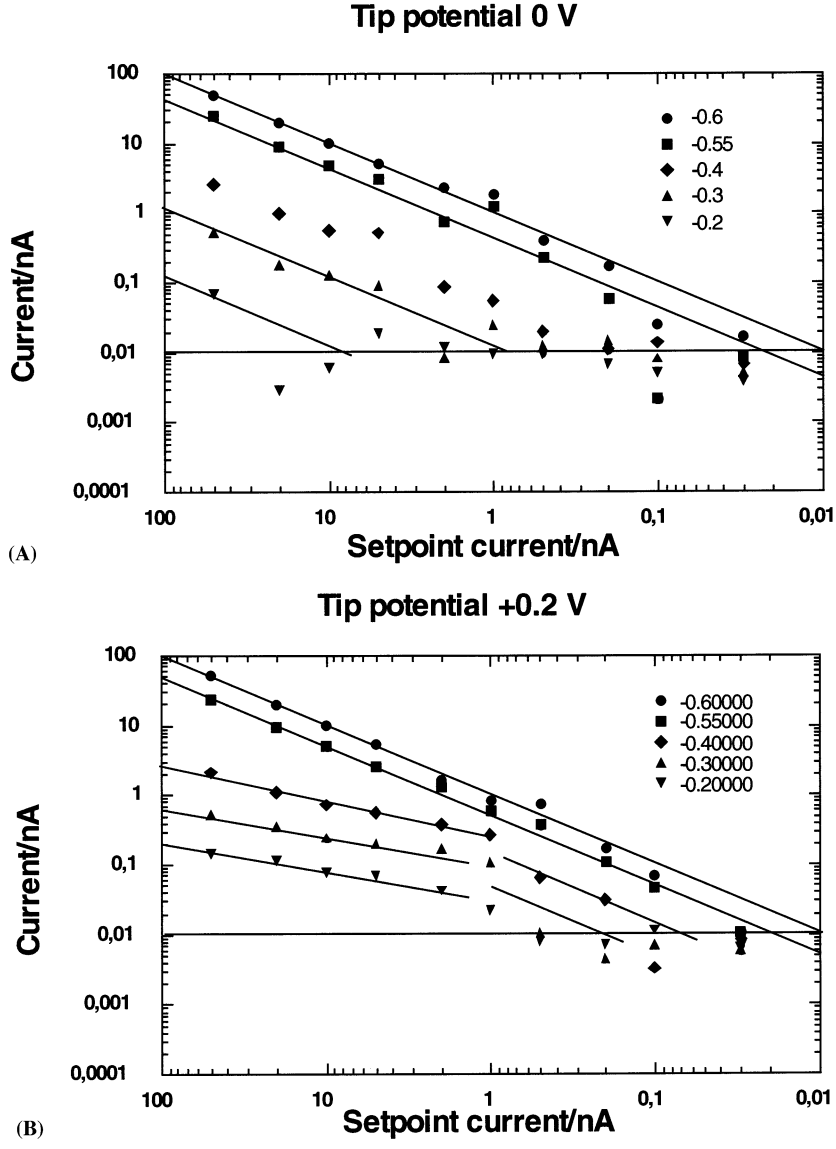

Fig. 8. Logarithmic plot of the tunneling current through the tip measured in 0.01 m H_2SO_4 plotted versus the setpoint currents for different semiconductor potentials and a tip potential of (a) 0 V; (b) +0.2 V; (c) +0.4 V; and (d) −0.2 V.

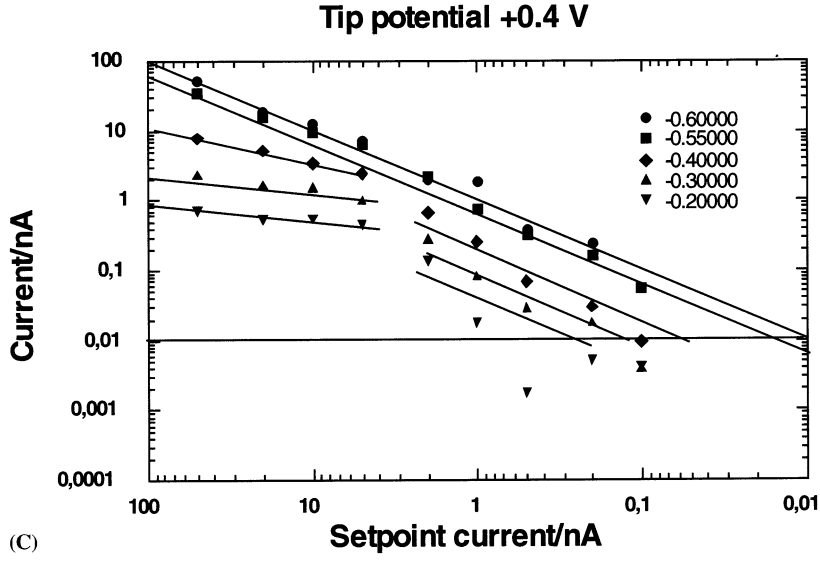

(C)

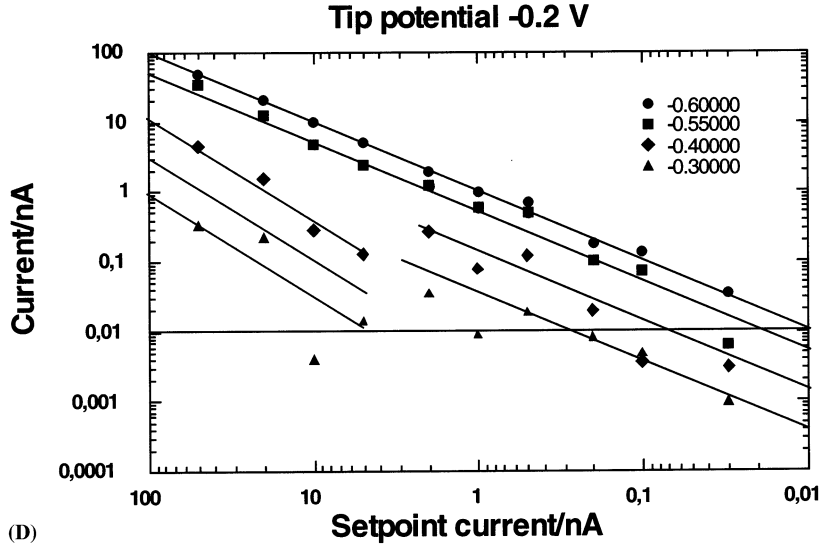

(D)

Fig. 8. (*Continued*)

electrolyte only (without assuming an additional barrier at the semiconductor surface). At large distances (smaller setpoint currents), the different curves have about the same slope as the reference line and the tunneling barrier thus determines the currents. Starting from a potential of -0.4 V going to more positive values, the current–distance curves expose a change in their slope leading to a smaller rise (and lower current values) for the larger setpoint currents. The absolute value of the current is larger than before, the barrier seems to be smaller for smaller distances. In Fig. 8c current–distance curves for a more positive tip potential of $+0.4$ V are given. A similar behavior can be found here. At larger distances the barrier is the same for all potentials but at smaller distances, also a change of the slope is occurring for the curves recorded at semiconductor potentials more positive than -0.4 V. The resulting slope of the curves for smaller distances to the semiconductor surface is even smaller compared to Fig. 8b, indicating an even smaller barrier but also with larger absolute current values. In Fig. 8d, the same evaluation has been made for a tip potential of -0.2 V. The setpoint current is again represented by the upper curve. Here, the opposite behavior is observed. At about the same distance between tip and sample (the same setpoint current), a change of the slope occurs, however, this time in the opposite direction. In this case, the slope of the current–distance curves is larger for the smaller distances than for the reference curve and the current has at first a smaller absolute

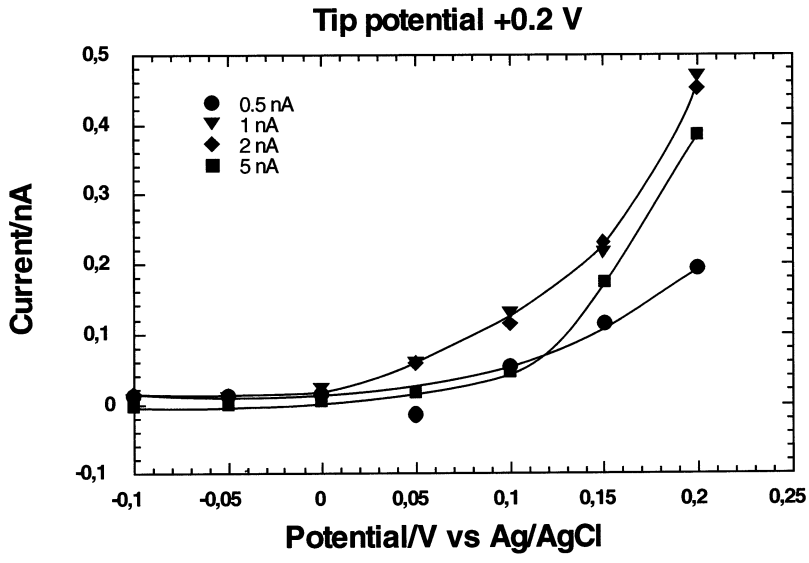

Fig. 9. Plot of the tunneling current through the tip vs. the semiconductor potential for different setpoint currents and a tip potential of +0.2 V in 0.0 1 m H_2SO_4

value. This is indicating a higher barrier at smaller distances.

From the above results we conclude that we can derive the influence of the two barriers, the tunneling barrier and the barrier at the semiconductor surface, on the tunneling current from the distance change of the current. For larger distances the barrier derived from the slope of the semilogarithmic plot of the current–distance curves is the same as the reference barrier, which is assumed to be determined by the tunneling barrier over the gap only. For smaller distances the barrier height is different from that at larger distances. In addition, we find that the change of this barrier seems to be connected to the potential of the tip becoming smaller for more positive tip potentials. This fact indicates that there is an electronic influence of the tip potential on the potential of the semiconductor that can be detected by the tunneling current. Its influence on the semiconductor/electrolyte barrier depends on the tip potential with respect to the electrolyte. For potentials positive of the point of zero charge (pzc) the barrier is decreased when the tip gets close to the semiconductor surface (it enters the electrochemical double layer) whereas the barrier is increased for tip potentials negative of its pzc. This behavior will be analyzed in more detail in a subsequent paper.

7. Hole current

In Fig. 9, a current–potential curve measured with a tip potential of +0.2 V is shown. Here, the current measured between the tip and semiconductor for positive semiconductor potentials is plotted. The magnitude of this current is the same for the substrate to tip distances determined by the setpoint currents of 1, 2 and 5 nA and is independent of the tip potential. The height of the current is obviously not limited by tunneling.

Here the current is determined by the hole current in the valence band, i.e. the number of holes available in the valence band of the semiconductor. This number is only dependent on the potential of the WSe_2. Since the current measured here is much smaller than the possible tunneling current, it is not limited by the tunneling distance. Only the curve measured at a distance corresponding to a setpoint current of 0.5 nA differs from this behavior. Here, the measured current is significantly smaller than for the larger distances. At this distance, the tunneling transmission factor becomes important and the currents are smaller according to the tunneling transmission over the barrier. The same has been found for the distance dependence of the photocurrent at this semiconductor. Due to the photogenerated charge carriers, holes are present at the surface and the measured tunneling current consists of electrons tunneling from the tip to the semiconductor. Here, it has also been found that the short circuit photocurrent is independent of the distance between the tip and semiconductor surface within to a certain distance range [2,9]. This property is typical for MIS (metal–insulator–semiconductor) solar cells, where the tunneling gap is filled by an oxide (or a solution as in our case) instead of vacuum, but where the transport of charge carriers is still determined by tunneling [18].

8. Summary and conclusion

The measurement of current–potential curves with a scanning tunneling microscope in an electrochemical cell has been analyzed in detail. Measurements of current–potential curves for different tunneling gaps and different potentials of the tip and the semiconductor have been recorded. An evaluation of the current–distance changes provides the possibility to distinguish between the barrier in the electrolyte and the barrier at the semiconductor/electrolyte interface. In addition, for a close contact between the tip and the semiconductor (when the electrochemical double layers of tip and semiconductor penetrate each other), an influence of the potential of the tip on the barrier height in the semiconductor has been found. This allows directly analysis of the structure of the electrochemical double layer that will be described in a forthcoming paper.

Acknowledgements

Financial support by the Volkswagen Foundation under contracts no. I/72 365, I/71902 and by the Deutsche Forschungsgemeinschaft under contracts no. ME855/3-1 and STI 74/9-2 is gratefully acknowledged. We are very grateful to Professor Levy, EPFL Lausanne, Professor Lux-Steiner, Dr Alonso-Vante and Y. Tomm, HMI Berlin, for providing semiconductor samples. Considerable support of this work by Professor Ulrich Stimming, TU München, is gratefully acknowledged.

References

[1] G. Binning, H. Rohrer, Helv. Phys. Acta 55 (1982) 726.
[2] R. Hiesgen, D. Meissner, Fres. J. Anal. Chem. 358 (1997) 54.
[3] R. Hiesgen, D. Meissner, Adv. Mater. 10 (1998) 619.
[4] R. Hiesgen, D. Meissner, J. Phys. Chem. 102 (1998) 6549.
[5] Y. Nosaka, K. Norimatsu, H. Myama, Chem. Phys. Lett. 106 (1984) 128.
[6] Y. Nakato, K. Ueda, H. Yano, H. Tsubomura, J. Phys. Chem. 92 (1988) 2316 and references cited therein.
[7] A. Maier, I. Uhlendorf, D. Meissner, Electrochim. Acta 40 (10) (1995) 1523.
[8] F.R.F. Fan, A. Bard, J. Phys. Chem. 97 (1993) 1431.
[9] R. Hiesgen, D. Meissner, Electrochim. Acta 42 (1997) 2881.
[10] C.E. Bach, R.J. Nichols, W. Beckmann, H. Meyer, A. Schulte, J. O. Besenhard, P.D. Jannakoudakis, J. Electrochem. Soc. 140 (1993) 1281.
[11] C. Hamann, W. Vielstich, Elektrochemie, third ed., Wiley-VCH, Weinheim, 1998.
[12] C. Sinn, PhD thesis, Hamburg, 1989.
[13] A. Uruchamy (Ed.), in: Photoelectrochemistry and Photovoltaics of Layered Semiconductors, Kluwer Academic, Dordrecht, 1992.
[14] W. Schmickler, Recent progress in theoretical electrochemistry, Ann. Rep. Sect. C 95 (1999) 117.
[15] W. Schmickler, D. Henderson, J. Electroanal. Chem. 290 (1990) 283.
[16] W. Jaegermann, private communication.
[17] R.D. Young, J. Ward, F. Scire, Phys. Rev. Lett. 27 (1971) 922.
[18] H.C. Card, Solid-State Electron. 20 (1977) 971.